

# Ordered Structures and Phase Transitions in Mixtures of a Polystyrene/Polyisoprene Block Copolymer with the Corresponding Homopolymers in Thin Films and in Bulk

Tetyana A. Mykhaylyk,\* Oleksandr O. Mykhaylyk, Stephen Collins, and Ian W. Hamley

Department of Chemistry, University of Leeds, Leeds LS2 9JT, UK

Received November 24, 2003; Revised Manuscript Received January 23, 2004

**ABSTRACT:** Microdomain structures and phase transitions of binary and ternary mixtures of polystyrene–polyisoprene–polystyrene (PS–PI–PS) triblock copolymer Vector 4111 (containing 18% PS) and the corresponding homopolymers were investigated in thin films by atomic force microscopy and in bulk by small-angle X-ray scattering. The neat copolymer shows a hexagonally packed cylinder structure. The addition of PI homopolymer caused a transition from the cylindrical to a spherical microdomain structure via a biphasic intermediate state with coexisting cylindrical and spherical domains for both thin films and bulk. In contrast, addition of a small amount (14 wt %) of minority-component PS homopolymer in a mixture leads to a significant increase of the cylindrical microdomain curvature in thin films. The influence of the added homopolymer PS on the structure of bulk samples is discussed. Addition of equal amounts of both components together does not change the cylindrical structure for bulk or thin film samples but results in an aligned cylindrical microdomain structure observed for thin films. Interdomain distances decreased upon addition of small or moderate amounts (7–38 wt %) of either or both homopolymer.

## 1. Introduction

It is now firmly established that the addition of a homopolymer to a block copolymer may cause changes in microdomain structure in the block copolymer.<sup>1</sup> In such blends there is an interplay between macrophase separation of the homopolymers and microphase separation of the block copolymer. Which effect predominates depends on the relative lengths of the polymers and on the composition of the blend. The key parameters controlling the microdomain morphology in blends of block copolymers consisting of A and B domains and a homopolymer A (HA) or/and B (HB) are  $r_A = N_{HA}/N_A$  and  $r_B = N_{HB}/N_B$ , where  $N_A$  and  $N_B$  are the degrees of polymerization of A and B block chains, respectively, and  $N_{HA}$  and  $N_{HB}$  are the degrees of polymerization of HA and HB, respectively.<sup>2</sup> Three extremes of the possible mixing states after phase separation are possible: (1) wet brush regime when  $r_A \ll 1$ ,  $r_B \ll 1$ ; (2) dry brush regime when  $r_A \approx 1$ ,  $r_B \approx 1$ ; and (3) macrophase separation when  $r_A \gg 1$ ,  $r_B \gg 1$ . These three regimes have different features and phase behavior. In the wet brush regime low molecular weight homopolymer tends to be selectively and uniformly solubilized into the corresponding block copolymer microdomain, swelling the block chains, and potentially causing changes in the initial microdomain morphology. In the dry brush regime added homopolymer tends still to be solubilized selectively into the corresponding microdomains but at the same time tends to localize in the middle of it and does not significantly swell the corresponding block chains. As a result, the addition of homopolymer in the dry brush regime does not substantially affect the initial morphology of the neat block copolymer although it may increase the interdomain spacing.<sup>2</sup>

Numerous studies have appeared on the phase behavior and phase transitions of block copolymer–homopolymer mixtures in all regimes. Most thin film studies have focused on symmetric diblock copolymers having lamellar microdomains.<sup>3–6</sup> The distribution of homopolymers and changes in lattice spacing have been quantitatively described. The behavior in thin film and in bulk of mixtures of an asymmetric diblock copolymer with a homopolymer has been studied as well.<sup>7,8</sup> An atomic force microscopy investigation of thin films of an asymmetric diblock copolymer<sup>7</sup> concentrated on changes in the domain spacing rather than phase transitions. Many studies on triblock copolymers have been concerned with the bulk behavior of almost symmetric copolymers having a lamellar morphology blended with midblock associating homopolymer.<sup>9–11</sup> Lamellar swelling induced by homopolymer has been characterized. Temperature-dependent bulk phase transitions have been investigated in binary blends consisting of the highly asymmetric triblock copolymer (Vector 4111) and the end block associating homopolymer polystyrene.<sup>12</sup> Recently we investigated the thin film morphology of blends of an asymmetric triblock copolymer with the corresponding homopolymers.<sup>13</sup> It is well-known that the phase behavior of the same block copolymers can differ dramatically in thin films and in bulk.<sup>6,14</sup> Here we extend our investigation to compare directly the behavior of the same copolymer/homopolymer blends in thin films and in bulk. Extremely low molecular weight homopolymers were chosen to ensure the uniform and selective solubilization of homopolymers in microdomain spaces of the corresponding blocks.

In this study, ordered structures and phase transitions of asymmetric block copolymer having cylindrical microdomains were investigated upon addition of homopolymers (midblock associating as well as end block associating and both together) in the wet brush regime for both thin films and bulk.

\* To whom correspondence should be addressed: e-mail T.A.Mykhaylyk@leeds.ac.uk.

**Table 1. Sample Code and Characteristics for the Block Copolymer Blends Investigated**

label	components (wt %)			total vol fraction, PS <sup>a</sup>	total vol fraction, PI <sup>a</sup>
	Vector 4111	homoPS	homoPI		
Vector 4111	100	0	0	0.16	0.84
86/14-PS	86	14	0	0.27	0.73
73/27-PS	73	27	0	0.37	0.63
62/38-PS	62	38	0	0.46	0.54
49/51-PS	49	51	0	0.56	0.44
93/07-PI	93	0	7	0.15	0.85
86/14-PI	86	0	14	0.14	0.86
73/27-PI	73	0	27	0.12	0.88
62/38-PI	62	0	38	0.10	0.90
93/07-PS/PI	93	3.5	3.5	0.18	0.82
86/14-PS/PI	86	7	7	0.20	0.80
73/27-PS/PI	73	13.5	13.5	0.24	0.76
62/38-PS/PI	62	19	19	0.27	0.73

<sup>a</sup> Volume fraction was estimated using the densities 1.05 and 0.91 g/cm<sup>3</sup> for PS and PI, respectively.<sup>21</sup>

## 2. Experimental Section

A commercially available polystyrene–polyisoprene–polystyrene (PS–PI–PS) block copolymer Vector 4111 (Dexco Polymers Co.) was used. Vector 4111 contains >99% triblock and 18 wt % (15.6 vol %) PS and has a number-average molecular weight ( $M_n$ ) of 128 000 g mol<sup>-1</sup> and a polydispersity ( $M_w/M_n$ ) of 1.11. Low molecular weight polystyrene (PS) (Alfa Aesar) having  $M_w = 1300$  and  $M_w/M_n = 1.06$  and low molecular weight polyisoprene (PI) (Polymer Source) having  $M_w = 1280$  and  $M_w/M_n = 1.11$  were used in the blends. All the polymers and chemicals were used without further purification.

Samples were prepared by first dissolving a predetermined amount of PS–PI–PS and PS and/or PI in toluene (2 wt % in solution) in the presence of 0.1 wt % of antioxidant (2,6-di-*tert*-butyl-*p*-cresol, Fluka). Then thin film samples for AFM investigations were spin-coated from the solution onto silicon wafers at 2000 or 6000 rpm. Film thicknesses were measured by a phase-modulated spectroscopic ellipsometer (Beaglehole Instruments). Samples were annealed in a vacuum oven at 130 °C and then quick quenched to room temperature. From our preliminary investigations we found that 3 h annealing time provided the best quality of thin block copolymer films produced and gave repeatable morphology so all samples in this study were annealed for 3 h.

We used the same solutions for preparation of bulk and thin film samples. Table 1 gives a summary of sample codes and composition used. It is well-known<sup>15</sup> that in thin films the polymer–air interface will be covered by a thin layer of the lower surface energy polymer (PI in our case) so the actual volume fraction of PI in microdomains in the interior of the film might be slightly lower for thin films. It should be noted here that all investigated samples were transparent in appearance without any turbidity: this indicates the absence of macrophase separation for the investigated range of compositions.

Bulk samples for small-angle X-ray scattering (SAXS) experiments were prepared by slowly evaporating the solvent at room temperature. The drying of the samples was continued until there was no further change in weight, and then the specimens were annealed in a vacuum oven for 3 h at 130 °C and stored in a refrigerator before experiments.

Tapping mode AFM (Nanoscope III, Digital Instrument) was used to image thin film samples spin-coated onto Si wafers. The AFM was operated under ambient conditions with commercial silicon microcantilever probe tips. Manufacturer's values for the probe tip radius and force constant are better than 10 nm and in the range 31–71 N/m, respectively. Topographic and phase images were obtained simultaneously using a resonance frequency of approximately 165 kHz for the probe oscillation; however, only the phase images are presented as they had more contrast. AFM characterization was performed immediately after annealing.

Small-angle X-ray scattering (SAXS) experiments were performed at the Synchrotron Radiation Source, Daresbury Lab, UK, on station 16.1 with a small-angle camera length 5.5 m and wavelength of X-ray radiation  $\lambda = 1.41$  Å. A 2D area detector (RAPID) was used to record SAXS patterns. Wet rat-tail collagen was used to calibrate the small-angle camera. A pseudo-Voigt function has been used in fitting to determine  $q$  values ( $q = 4\pi \sin \theta/\lambda$ , where  $2\theta$  is the scattering angle) of observed Bragg peaks.

To check the order–disorder transition (ODT) temperature  $T_{ODT}$ , some samples were placed in TA Instruments differential scanning calorimeter (DSC) pans, modified for transmission of X-rays by the insertion of mica windows. The pan was heated and cooled in a Linkam DSC of single-pan design. Heating ramps were performed in the temperature interval 100–220 °C at a rate of 4 °C/min.

## 3. Results and Discussions

To obtain well-defined microphase-separated ordered structures upon annealing of a block copolymer, the annealing temperature should be lower than  $T_{ODT}$  of the block copolymer (or lattice disordering/ordering transition (LDOT) temperature  $T_{LDOT}$  in the terminology proposed by Han et al.<sup>16</sup> for highly asymmetric block copolymers) but above the glass transition temperature  $T_g$  of glassy block. It is established (at least for PS) that the glass transition temperature decreases as the thickness of the film is reduced.<sup>17</sup> However, the relationship between  $T_{ODT}$  in bulk systems and in thin films is rather complicated and still remains open to question. For example, surface-induced order was found far above the bulk order–disorder transition temperature<sup>18</sup> for a symmetric *d*PS–PMMA [PMMA = poly(methyl methacrylate)] copolymer and the temperature  $T_{\infty}$ , at which the film was still fully ordered, increased with decreasing film thickness, and remained above  $T_{ODT}$  for the whole range of thicknesses of a symmetric PS–*d*PMMA block copolymer.<sup>19</sup> On the other hand, for a monolayer of spheres formed by an asymmetric PS–P2VP [P2VP = poly(2-vinylpyridine)] diblock copolymer, the hexatic-to-isotropic liquid transition temperature of the 2D block copolymer film was significantly lower than the 3D block copolymer  $T_{ODT}$ .<sup>20</sup> Taking into account possible ambiguities in results concerning  $T_{ODT}$  for thin films, we will refer below to  $T_{ODT}$  values for bulk samples only.

We choose an annealing temperature of 130 °C, which lies between  $T_g$  (polystyrene)  $\sim 100$  °C<sup>21</sup> and  $T_{ODT}$  (Vector 4111). Vector 4111 undergoes an ODT at temperatures between 210 °C (onset) and 214 °C (completion).<sup>22</sup> Several experimental studies reported that the addition of low molecular weight homopolymers to block copolymers decreases the temperature of the order–disorder transition  $T_{ODT}$ ;<sup>12,23</sup> thus, we selected the annealing temperature far below  $T_{ODT}$  of neat Vector 4111. Although the detailed investigation of the  $T_{ODT}$  of block copolymer/homopolymer blends is out of the scope of this paper, we performed SAXS measurements upon heating of the bulk blends up to 220 °C to check  $T_{ODT}$  for the blends used in our study. For all blends investigated, except 49/51-PS, the  $T_{ODT}$  was above 130 °C.

**3.1. Neat Block Copolymer.** The bulk morphology of Vector 4111 is characterized by a set of Bragg peaks corresponding to a hexagonal (hex) structure (Figure 1, Table 2). This indicates that the PS component of the copolymer forms cylinders surrounded by a PI matrix.<sup>12,22</sup> A representative AFM image of a thin film of neat Vector 4111 shows a “fingerprint” structure formed by parallel domains (Figure 2). Although AFM images represent only the surface of the film and provide no





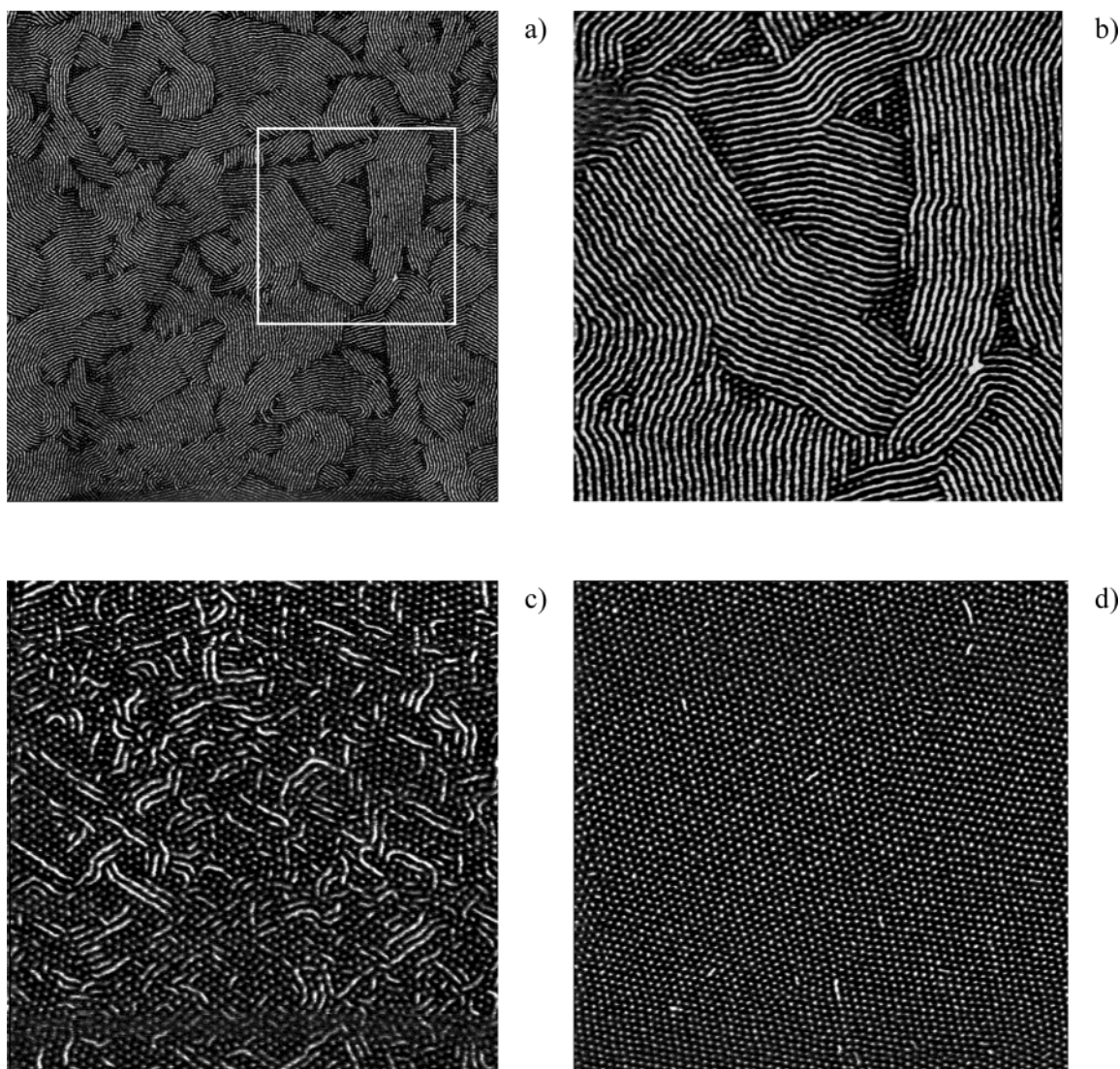


**Figure 3.** AFM image (phase contrast) of the Vector 4111/PI mixture: (a) 7 wt % PI homopolymer added ( $5\ \mu\text{m}$  scale); (b) (enlarged portion of (a)) 7 wt % PI homopolymer added ( $1.84\ \mu\text{m}$  scale); (c) 14 wt % PI homopolymer added ( $2\ \mu\text{m}$  scale); (d) 27 wt % PI homopolymer added ( $2\ \mu\text{m}$  scale).

pure triblock films. All AFM images presented are for thicker films (obtained by spin-coating at 2000 rpm). The bright and dark areas in the image correspond to PS cylinders and PI matrix, respectively, as PS has a higher modulus than PI.

**3.2. Microdomain Structures and Phase Transitions in Vector 4111/PI Blends.** At least two ordered phases are recognizable in SAXS patterns obtained for Vector 4111 + PI blends (Figure 1). Even a small amount of the homopolymer in the sample (7 wt %) leads to the appearance of extra peaks coexisting with those for the hexagonal structure of neat Vector 4111. The extra peaks become more intense as the amount of added PI homopolymer increases (14 wt %), and all of them can be indexed to a body-centered-cubic (bcc) structure (Figure 1, Table 2). It has to be noted that the presence of a Bragg peak at a relative position  $q/q^* = \sqrt{7}$  (where  $q^*$  is the position of the first-order peak) enables the observed diffraction pattern to be distinguished from that of a primitive cubic cell. Thus, SAXS measurements reveal that the presence of PI homopolymer in the blend causes a transformation of hexagonally packed cylindrical PS microdomains into spherical ones packed in a body-centered-cubic lattice.

The explanation of the increase in the interfacial curvature of PS domains that accompanies this transition is as follows.<sup>2</sup> To retain normal liquid-state densities on addition of PI homopolymer while maintaining constant curvature, the PI block must stretch and/or the PS block contract. However, an alternative is for the interface to curve, and this is usually favored because it involves less conformational entropy loss.

A further increase of PI concentration in the blend (27 and 38 wt %) leads to a smearing of the Bragg peaks, indicating the formation of a poorly ordered structure within the blend. The observed SAXS patterns contain features of both structure factor and form factor. There are three broad peaks. The peak with the lowest  $q$  value located at the position of the cubic 011 reflection and the other two peaks located respectively within regions of two groups of cubic reflections 002, 112 and 013, 222, 123 indicate that a motif of cubic packed PS microdomains formed at a lower concentration of PI homopolymer still remains in the structure. However, this is only local order and the peak at the highest  $q$  value could also be related to the first order of a form factor of spheres. Considering the volume fractions of domains,<sup>29</sup> the estimated radius of PS spheres ( $R_s$ ) is equal

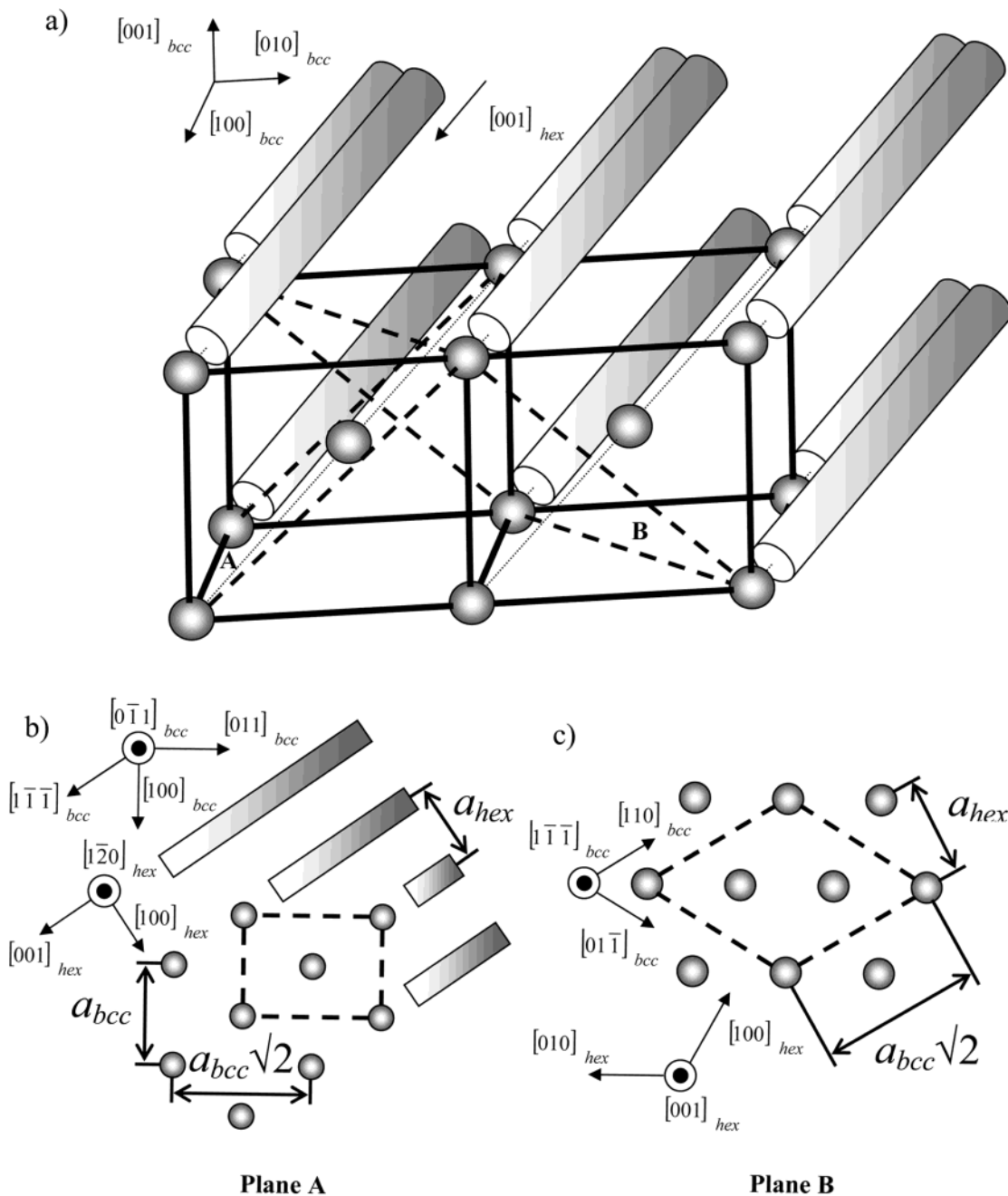


**Figure 4.** Transition from cylinders to spheres in bulk (a). Cross section A represents a structure observed by AFM at the surface of a thin film (b). Cross section B shows a hexagonally packed structure (c). The dashed quadrangles show orientation of the cross-section planes.

to 92.5 and 87.5 Å for 27 and 38 wt % of PI, respectively. Thus, from the position of the first maximum in the Bessel function  $J_{3/2}$  that defines the form factor of uniform spheres at  $qR_s = 5.765$ <sup>30</sup> the position of the first maximum in the SAXS pattern is expected at  $q = 5.765/92.5 \text{ Å} = 0.062 \text{ Å}^{-1}$  and  $q = 5.765/87.5 \text{ Å} = 0.066 \text{ Å}^{-1}$  for 27 and 38 wt % of PI, respectively. These values are quite close to the position of the third maximum observed in the SAXS patterns (Figure 1).

AFM investigations for thin film samples reveal a morphological transition from cylinders (Figure 2) to spheres (Figure 3d) on increasing the total volume fraction of PI from 0.84 to  $\geq 0.88$ , as for bulk samples. As AFM can probe only the top layer of the films, the observed hexagonally packed dots for the blend containing 27 wt % PI (Figure 3d) could equally be interpreted as spheres or as ends of cylinders perpendicular to the

substrate in the absence of information on order perpendicular to the substrate. The clear evidence for a cubic structure for bulk samples enables us to assume that the hexagonally packed dots observed in the thin film are spheres and not cylinder ends.

In thin films a biphasic intermediate state with coexisting cylindrical and spherical domains was observed (Figure 3a,b) for blends with an intermediate amount of PI homopolymer (7 wt %), in agreement with SAXS data. The main features of this structure are (i) the appearance of a "patchwork quilt" effect (Figure 3a) consisting of grains containing cylinders aligned (mostly) in parallel stripes but with sharp grain boundaries that can have large tilt angles and (ii) the apparent nucleation of spheres at grain boundaries in an epitaxial relationship to cylinders.<sup>31</sup>



A mechanism for the epitaxial transition in films (or endotaxial transition in a body) between hexagonally packed cylinders and bcc packed spheres has previously been proposed,<sup>32</sup> and a schematic three-dimensional representation of these two structures is illustrated in Figure 4a for convenience. The cross section in plane A (Figure 4b) corresponds to a structure which is visible by AFM on the surface of the thin film (Figure 3b). One can see nearly hexagonally packed spheres epitaxially formed from cylinders. The cross section in plane B represents a different projection showing a hexagonal configuration (Figure 4c).

As for the bulk sample, the film with a PI volume fraction of 0.86 appears to be at a boundary point between the biphasic intermediate state and the sphere morphology (Figures 3c and 1). Upon further addition of PI homopolymer thin films and bulk show different behavior. Although large PI homopolymer concentration in bulk caused a poorly ordered state, thin films showed well-ordered structures up to the maximum PI homopolymer concentration used. Such a discrepancy in the behavior in thin film compared to bulk could be explained taking into account a confinement effect for thin films. It was found that the constraints imposed by the finite film thickness led to surface-induced ordering in thin films of both symmetric<sup>18,19</sup> and asymmetric<sup>33</sup> block copolymers. Surface fields (propagating from both air and substrate interface) effect could be so strong that the surface-induced effect persists even above the bulk order–disorder transition.<sup>19</sup>

**3.3. Microdomain Structures and Phase Transitions in Vector 4111/PS Blends.** A moderate concentration of PS homopolymer (14 wt %) in a blend with Vector 4111 does not change the hexagonal packing of PS microdomains observed for pure copolymer (Figure 5). However, at higher concentration of PS homopolymer (27 wt %) a bulk sample demonstrates different SAXS patterns (Figure 5). There are four peaks which might be identified as a hexagonal structure ( $q:q^* = \sqrt{1}:\sqrt{4}:\sqrt{7}:\sqrt{9}$ , Table 2), but the absence of a peak at  $q/q^* = \sqrt{3}$  makes this interpretation problematic. Similar scattering intensity profiles have recently been observed during the order–order transition between hexagonal and gyroid phases of diblock copolymer/homopolymer blends<sup>34</sup> and were ascribed to an intermediate structure. We will follow this point of view. A lamellar structure is expected at higher PS concentration in the blend,<sup>12</sup> and the observed patterns of four peaks may point to a hexagonal–lamellar phase transition which proceeds via an intermediate structure. Further increase of PS homopolymer in the blend leads to formation of a disordered structure, which is clearly indicated by the absence of high-order diffraction maxima in the SAXS patterns. Similar Vector 4111/PS blends have been investigated recently by Vaidya et al.<sup>12</sup> They found from TEM that at room temperature 86/14 and 73/27 blends have a hexagonally packed cylindrical microdomain structure and 62/38 whereas 49/51 blends have lamellar microdomain structure. Our results agree clearly for the 86/14 blend that forms hexagonally packed cylinders. For a 62/38 blend we observed clear lamellar ordering only at high temperature.

As one can see in Figure 6a for the 86/14-PS thin film sample, the addition of a small amount of minority-component PS homopolymer (14 wt %) results in a morphology that still comprises PS cylinders but also shows some significant features not visible for neat

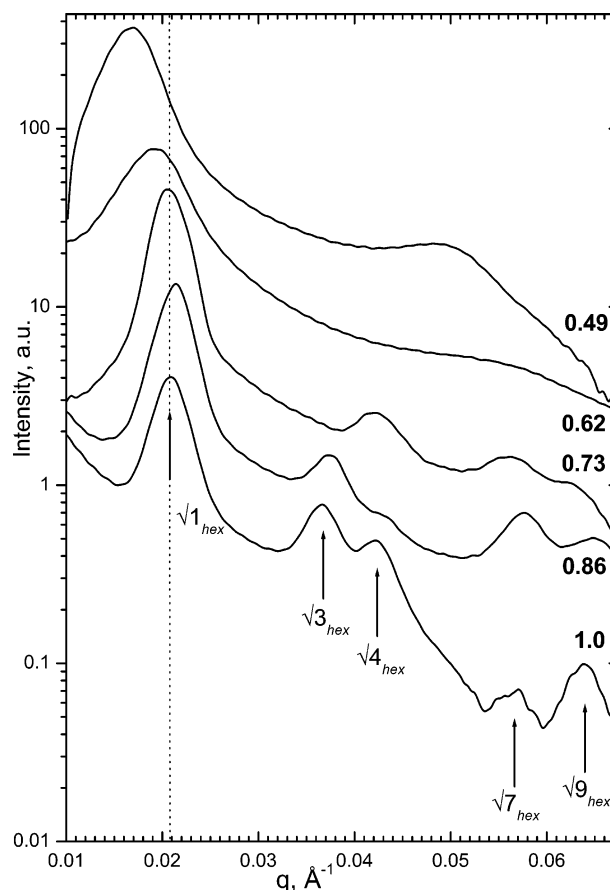


**Figure 5.** SAXS profiles as a function of wt % of Vector 4111 in bulk mixtures with PS homopolymer. The SAXS profiles were shifted vertically to avoid overlap.

Vector 4111. It can be characterized by the integration of former cylinders into a PS network (brighter areas) and a significant increase in the curvature of the remaining PS cylinders.

A rather complicated surface morphology appears in thin films upon addition of 27 wt % PS (Figure 6b). It could be characterized as a majority of bright connected PS domains with a small amount of disordered dark areas corresponding to the PI component. Following the SAXS results, this structure can be characterized as a transient state from the cylindrical to the lamellar morphology. It should be noted here that further addition of PS homopolymer (62/38-PS and 49/51-PS) does not change significantly the morphology of thin film samples. The AFM images (not reproduced here) were similar to Figure 6b, i.e., showing an irregular structure with a majority of connected PS domains. Another possible explanation of this structure could be proposed taking into account that for 49/51-PS  $T_{ODT}$  is equal to 105 °C.<sup>12</sup> Then annealing at 130 °C will produce “micelles without long-range order”, and upon quenching to room temperature this morphology is trapped. In the AFM image, the dark disordered spots then represent frozen PI micelles in the PS matrix.

**3.4. Microdomain Structures and Phase Transitions in Vector 4111/(PS + PI) Blends.** Addition of a moderate amount of both homopolymers together (50:50 proportion) in a blend with Vector 4111 does not change the structure from that of the pure copolymer. Five peaks corresponding to a hexagonal structure are evident in SAXS patterns for blends containing 7 and 14 wt % of the homopolymers (Figure 7). A higher

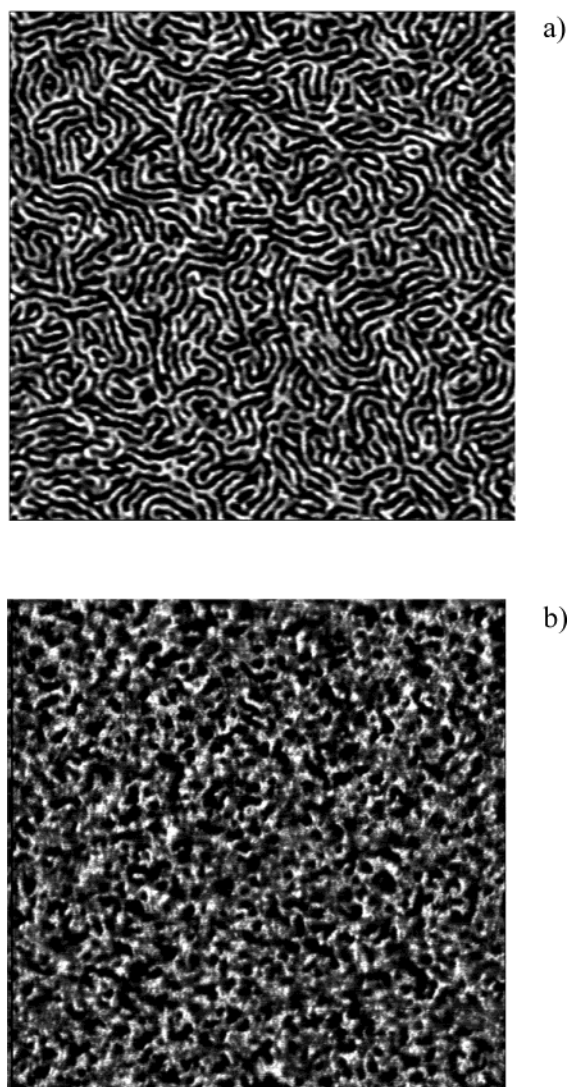


**Figure 6.** AFM image (phase contrast) of the Vector 4111/PS mixture: (a) 14 wt % PS homopolymer added; (b) 27 wt % PS homopolymer added (2  $\mu\text{m}$  scale).

concentration of the homopolymers in the blends leads to the formation of a disordered structure indicated by smeared diffraction features. There are three broad peaks. The first one characterized by the lowest  $q$  value could be relevant to the first-order 010 peak of the hexagonal structure. The second one could be a product of a superposition of broadened 110 and 020 peaks. The third peak could be either a product of broadened 120 and 030 peaks or a result of a form factor of infinite cylinders. Considering the volume fraction of domains,<sup>29</sup> the estimated radius of PS cylinders ( $R_c$ ) is equal to 85.9 and 92.7  $\text{\AA}$  for 27 and 38 wt % PI/PS, respectively. The first subsidiary maximum in the form factor of infinite cylinders is at  $qR_c = 4.98$ .<sup>30</sup> Therefore, the position of the first maximum in the SAXS pattern has to be expected at  $q = 4.98/85.7 \text{ \AA} = 0.058 \text{ \AA}^{-1}$  and  $q = 4.98/92.7 \text{ \AA} = 0.054 \text{ \AA}^{-1}$  for 27 and 38 wt % PI/PS, respectively. The estimated  $q$  values are close to the position of the third maximum observed in the SAXS patterns, especially for the blend containing 27 wt % PI/PS (Figure 7).

Addition of equal amounts of both homopolymers together leaves a cylindrical microdomain structure for thin film samples (Figure 8a,b) as for bulk (Figure 7). Clearly, we can expect that in the wet brush regime, as

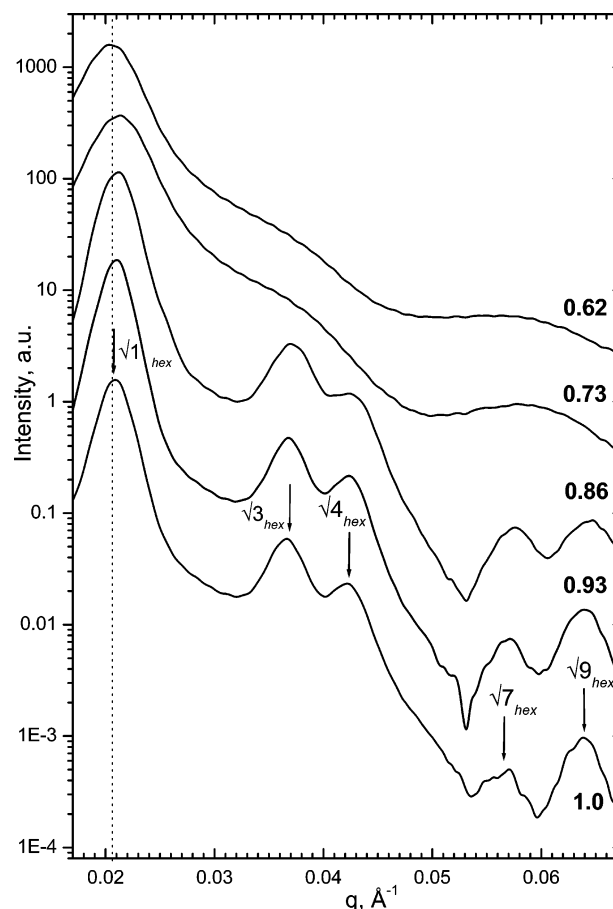


**Figure 7.** SAXS profiles as a function of wt % of Vector 4111 in bulk mixtures with PI and PS homopolymers. The SAXS profiles were shifted vertically to avoid overlap.

long as we do not exceed the critical PS concentration for the cylinder–lamellar phase transition, the cylindrical morphology will be conserved, and our results for bulk and thin film samples confirmed this.

An interesting observation for thin film samples was the alignment of cylindrical domain upon addition of the 50:50 mixture of homopolymers. The observed increase in alignment of the cylinders may be due to a reduction in pinning of defects in the stripe pattern<sup>27</sup> on the substrate due to preferential segregation of PI to the substrate or alternatively due to “plasticization” by low molecular weight polymer “diluent” leading to a reduced viscosity and easier local alignment upon annealing.

**3.5. Interdomain Distance.** The interdomain spacing (in-plane order) was estimated for film samples by Fourier transformation of AFM images (Table 3). One can see that for *all* blends the interdomain distance *decreases* with the addition of homopolymer. The effect of domain contraction upon addition of low molecular weight homopolymers was observed in bulk for lamellar phase triblock copolymer/homopolymer blends upon addition of low molecular weight midblock associated homopolymer<sup>35</sup> and for both lamellar<sup>36</sup> and cylindrical<sup>8</sup> diblock copolymer/homopolymers blends. The effect was also explained theoretically.<sup>37</sup> A low molecular weight homopolymer has a higher entropy of mixing in the corresponding block copolymer domain than a high molecular weight homopolymer. Low molecular weight homopolymer can penetrate throughout the block copolymer domain, causing an increase in interfacial area, producing a greater contraction in the opposite domain.



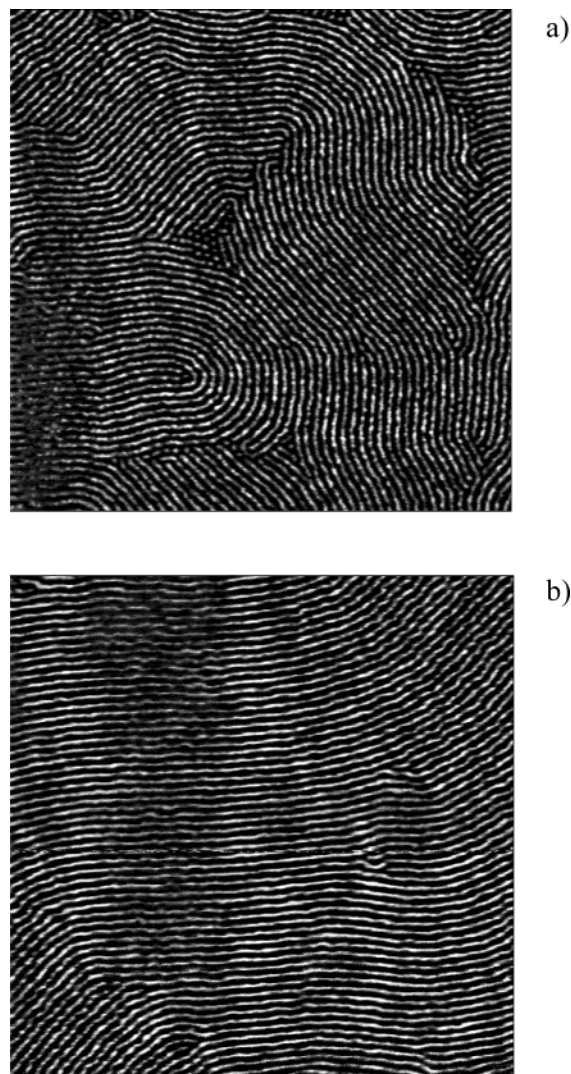


**Figure 8.** AFM image (phase contrast) of the Vector 4111/PI/PS mixture: (a) 14 wt % PS/PI (50/50) homopolymers added ( $2\ \mu\text{m}$  scale); (b) 27 wt % PS/PI (50/50) homopolymers added ( $1.68\ \mu\text{m}$  scale).

**Table 3.** Interdomain Distance  $D$  (Å) for Vector 4111/Homopolymer Blends Estimated for Thin Films

	Vector 4111 + PI		Vector 4111 + PS	Vector 4111 + PI + PS
	hex	cub		
93%	$420 \pm 10$			$340 \pm 10$
86%	$380 \pm 10$	$380 \pm 10$	$400 \pm 20$	$370 \pm 20$
73%		$340 \pm 20$		$320 \pm 10$
62%		$290 \pm 20$		$350 \pm 10$

This in turn causes the overall period to decrease.<sup>37</sup> Our observation confirmed the existence of a similar effect in thin films.

We performed additional measurements of thin film thickness for all blends (produced at the *same* spin speed) by ellipsometry and noticed a significant decrease in film thickness (down to 70% of the initial neat block copolymer film thickness) upon addition of homopolymer for *all* blend films. We discussed earlier the connection between thin film thickness and thin film morphology. Our thin systems do not show any terracing effect, so presumably to match the particular thickness after spin-coating the thin film structure experiences some distortion. Although the film thickness decrease is clear and could be explained by domain contraction, further

measurements are needed to probe changes in both in-plane and out-of-plane order.

The good agreement between the radius of cylindrical and spherical domains estimated from SAXS experiments and that calculated from the known volume fraction, assuming uniform selective solubility (sections 3.2–3.3) confirmed that the PI and PS homopolymers are all solubilized within the corresponding block microdomain.

#### 4. Conclusions

The addition of majority-component PI homopolymer to Vector 4111 caused a transition from a cylindrical to a spherical microdomain structure in bulk and in thin films. The intermediate state with biphasic coexistence between the cylindrical and the spherical phase showed that for thin films (i) formation of spheres starts from the boundary regions between clusters of cylinders and (ii) these two phases have a structural relationship and that spheres form epitaxially, following the direction of former cylinders. A detailed mechanism for this was presented.

The addition of a small concentration of minority-component PS homopolymer leads to an intermediate structure, a possible precursor to a lamellar phase. There are similarities between the scattering pattern for the 27 wt % PS blend and that previously observed close to the hexagonal-to-gyroid phase transition.<sup>34</sup>

Addition of a 50:50 blend of PI and PS homopolymers does not change the cylindrical morphology in bulk or in thin films and leads to enhanced alignment of cylinders parallel to the surface for thin films. This intriguing (and reproducible) phenomenon may be due to segregation of PI to the substrate forming an additional “wetting layer” or may be caused by “plasticization” of the PS by low molecular weight homopolymer.

Addition of low molecular weight homopolymers either separately or both together to an asymmetric triblock copolymer caused *contraction* of the domain spacing for thin films. No terrace formation was observed, pointing to uniform changes in film thickness (and consequent lateral contraction).

**Acknowledgment.** We thank the EPSRC for supporting T.M. (GR/N64793), O.M. (GR/N22052), and S.C. (GR/N00678). The authors thank the SRS, Daresbury Lab for assistance with SAXS experiments.

#### References and Notes

- (1) Hamley, I. W. *The Physics of Block Copolymers*; Oxford University Press: Oxford, 1998.
- (2) Hasegawa, H.; Hashimoto, T. In *Comprehensive Polymer Science*; Aggarwal, S. L., Russo, S., Eds.; Pergamon: London, 1996.
- (3) Orso, K. A.; Green, P. F. *Macromolecules* **1999**, *32*, 1087–1092.
- (4) Retsof, H.; Terzis, A. F.; Anastasiadis, S. H.; Anastassopoulos, D. L.; Toprakcioglu, C.; Theodorou, D. N.; Smith, G. S.; Menelle, A.; Gill, R. E.; Hadziioannou, G.; Gallot, Y. *Macromolecules* **2002**, *35*, 1116–1132.
- (5) Smith, M. D.; Green, P. F.; Saunders, R. *Macromolecules* **1999**, *32*, 8392–8398.
- (6) Green, P. F.; Limary, R. *Adv. Colloid Interface Sci.* **2001**, *94*, 53–81.
- (7) Jeong, U. Y.; Kim, H. C.; Rodriguez, R. L.; Tsai, I. Y.; Stafford, C. M.; Kim, J. K.; Hawker, C. J.; Russell, T. P. *Adv. Mater.* **2002**, *14*, 274–276.
- (8) Jeong, U.; Ryu, D. Y.; Kho, D. H.; Lee, D. H.; Kim, J. K.; Russell, T. P. *Macromolecules* **2003**, *36*, 3626–3634.



- (9) Norman, D. A.; Kane, L.; White, S. A.; Smith, S. D.; Spontak, R. J. *J. Mater. Sci. Lett.* **1998**, *17*, 545–549.
- (10) Kane, L.; Norman, D. A.; White, S. A.; Matsen, M. W.; Satkowski, M. M.; Smith, S. D.; Spontak, R. J. *Macromol. Rapid Commun.* **2001**, *22*, 281–296.
- (11) Roberge, R. L.; Patel, N. P.; White, S. A.; Thongruang, W.; Smith, S. D.; Spontak, R. J. *Macromolecules* **2002**, *35*, 2268–2276.
- (12) Vaidya, N. Y.; Han, C. D.; Kim, D.; Sakamoto, N.; Hashimoto, T. *Macromolecules* **2001**, *34*, 222–234.
- (13) Mykhaylyk, T. A.; Collins, S.; Hamley, I. W.; Evans, S. D.; Henderson, J. R. *J. Mater. Sci.* **2004**, *39*, 2249–2252.
- (14) Krausch, G. *Mater. Sci. Eng.* **1995**, *R14*, 1–94.
- (15) Turturro, A.; Gattiglia, E.; Vacca, P.; Viola, G. T. *Polymer* **1995**, *36*, 3987–3996.
- (16) Han, C. D.; Vaidya, N. Y.; Kim, D.; Shin, G.; Yamaguchi, D.; Hashimoto, T. *Macromolecules* **2000**, *33*, 3767–3780.
- (17) Keddie, J. L.; Jones, R. A. L.; Cory, R. A. *Europhys. Lett.* **1994**, *27*, 59–64.
- (18) Anastasiadis, S. H.; Russell, T. P.; Satija, S. K.; Majkrzak, C. F. *Phys. Rev. Lett.* **1989**, *62*, 1852–1855.
- (19) Menelle, A.; Russell, T. P.; Anastasiadis, S. H.; Satija, S. K.; Majkrzak, C. F. *Phys. Rev. Lett.* **1992**, *68*, 67–70.
- (20) Segalman, R. A.; Hexemer, A.; Hayward, R. C.; Kramer, E. J. *Macromolecules* **2003**, *36*, 3272–3288.
- (21) *Polymer Handbook*, 4th ed.; Brandup, J., Immergut, E. H., Grulke, E., Eds.; John Wiley: New York, 1998.
- (22) Sakamoto, N.; Hashimoto, T.; Han, C. D.; Kim, D.; Vaidya, N. Y. *Macromolecules* **1997**, *30*, 1621–1632.
- (23) Winey, K. I.; Thomas, E. L.; Fetters, L. J. *Macromolecules* **1992**, *25*, 2645–2650.
- (24) Mykhaylyk, T. A.; Collins, S.; Jani, C.; Hamley, I. W. *Eur. Polym. J.*, in press.
- (25) Harrison, C.; Park, M.; Chaikin, P.; Register, R. A.; Adamson, D. H.; Yao, N. *Macromolecules* **1998**, *31*, 2185–2189.
- (26) Segalman, R. A.; Schaefer, K. E.; Fredrickson, G. H.; Kramer, E. J.; Magonov, S. *Macromolecules* **2003**, *36*, 4498–4506.
- (27) Harrison, C.; Chaikin, P. M.; Huse, D. A.; Register, R. A.; Adamson, D. H.; Daniel, A.; Huang, E.; Mansky, P.; Russell, T. P.; Hawker, C. J.; Eglolf, D. A.; Melnikov, I. V.; Bodenschatz, E. *Macromolecules* **2000**, *33*, 857–865.
- (28) Karim, A.; Singh, N.; Sikka, M.; Bates, F. S.; Dozier, W. D.; Felcher, G. P. *J. Chem. Phys.* **1994**, *100*, 1620–1629.
- (29) From volumetric considerations for bulk samples, the radius of the PS spheres  $R_s$  and radius of the PS cylinders  $R_c$  can be estimated from the interdomain distance  $D$ , volume fraction of PS in Vector 4111 block copolymer  $f$ , and volume fraction of PI homopolymer  $\phi$  and PS homopolymer  $x$ :  $R_s = \{[3(1 - \phi)(1 - x)]/[8\pi(1 + \phi x)](f + (x/(1 - x)))^{1/3} D$ .  $R_c = \{[\sqrt{3}(1 - \phi)(1 - x)]/[2\pi(1 + \phi x)](f + (x/(1 - x)))^{1/2} D$ . We assume here that PS and PI homopolymers are selectively and uniformly solubilized into the corresponding block copolymer domains only (this assumption is valid in the wet brush regime).
- (30) Guinier, A. *Small-Angle Scattering of X-ray*; Wiley: New York, 1955.
- (31) Matsen, M. W. *J. Chem. Phys.* **2001**, *114*, 8165–8173.
- (32) Koppi, K. A.; Tirrell, M.; Bates, F. S.; Almdal, K.; Mortensen, K. *J. Rheol.* **1994**, *38*, 999–1027.
- (33) Liu, Y.; Zhao, W.; Zheng, X.; King, A.; Singh, A.; Rafailovich, M. H.; Sokolov, J.; Dai, K. H.; Kramer, E. J.; Schwarz, S. A.; Gebizlioglu, O.; Sinha, S. K. *Macromolecules* **1994**, *27*, 4000–4010.
- (34) Bodycomb, J.; Yamaguchi, D.; Hashimoto, T. *Macromolecules* **2000**, *33*, 5187–5197.
- (35) Quan, X.; Gancarz, I.; Koberstein, J. T.; Wignall, G. D. *Macromolecules* **1987**, *20*, 1431–1434.
- (36) Winey, K. I.; Thomas, E. L.; Fetters, L. J. *Macromolecules* **1991**, *24*, 6182–6188.
- (37) Matsen, M. W. *Macromolecules* **1995**, *28*, 5765–5773.

MA035758S